POLITECNICO
MILANO 1863

SCUOLA DI INGEGNERIA INDUSTRIALE
E DELL'INFORMAZIONE

Executive Summary of the Thesis

Modelling dislocation density evolution of UO_2 under irradiation

Laurea Magistrale in Nuclear Engineering - Ingegneria Nucleare

Author: Aleksandar Djonovic

Advisor: Prof. Lelio Luzzi

Co-advisor: T. Barani, D. Pizzocri

Academic year: 2023-2024

1. Introduction

Fuel performance codes have been mainly developed to predict fuel behaviour for conventional light water reactors (LWRs), which are the most common reactor type worldwide and for which decades of research have greatly supported their fuel modelling. However, future advanced modular reactor designs, such as small modular reactors dedicated to industrial heat production, lack this extensive feedback. In such concepts, the envisaged fuel temperature ($T_{fuel} < 250$°C) lies below the normal range encountered in commercial pressurized water reactors. Within this temperature range, attention has been drawn towards the formation of high burn-up structure (HBS) restructuring [1]. Various models describe the HBS phenomenon, with many indicating different modalities of restructuring. Commonly, these descriptions point to the accumulation of microstructural defects, emphasizing the role of dislocations in the restructuring process [2] [3] [4] [5]. This observation is supported by TEM images, in particular those derived by Nogita and Une [6], who identified the reorganization of grain boundaries into sub-divided grains (20–30 nm) with high angle boundaries as a result of stored strain energy release in the matrix. These microstructural modifications induced by prolonged irradiation damage have an impact on the fuel behavior between the pre- and post- restructuring. To properly predict fuel operation, fuel performance codes must account for this restructuring process. As part of the PLEIADES platform developed at CEA, fission gas modules like MARGARET [7] exploit the correlation developed from the experimental observations by Nogita and Une [6] as a simplified dislocation model to determine the morphological state in which the fuel should be described. However, as we move beyond the irradiation conditions of the reference fuel specimens, the current correlations may not be applicable to predict dislocation density and consequently the emergence of HBS. Therefore, current models may fail to predict fuel restructuring for novel reactor designs, while safety requirements need an accurate density dislocation prediction. To overcome the limitations imposed by empirical evaluations, more physical-based models are to be preferred since they are not dependent on the specific conditions at which certain experimental irradiation samples had been subjected.
With the purpose of developing a physics-based model for the evaluation of dislocation density in UO_2, it is necessary to integrate an accurate formulation of the phenomena governing the kinetics of the main microstructural features iden-

tified in the fuel. Rate theory modelling is an approach able to embed all these mechanisms in a set of coupled ordinary differential equations, and it has been traditionally applied to describe the microstructural evolution of materials under irradiation at the mesoscopic scale [8] [9]. In particular, the work by Veshchunov and Shestak [10] was taken as a starting reference since it one of the most exhaustive rate-theory models available in open literature devoted to the development of HBS restucturing. Nevertheless, this model suffers from heavy mathematical formulations that compromise its practical implementation. Instead, the presented work tries to avoid non-linear expressions and discontinuities which tend to worsen numerical performance, while integrating additional physical mechanisms for a more comprehensive description.

2. Model Equations

The model describes a kinetic system accounting for both point and extended defects with seven variables in the mean field approximation, for which all the defects are uniformly distributed within the material and their interactions occur continuously in space and time[1].
The temperature dependence of the model is mostly contained within the expressions for the uranium defects diffusivity $D_{v,i}$ $\left(\mathrm{m}^2 \cdot \mathrm{s}^{-1}\right)$. Diffusivity expressions determine how fast the defects will move and consequently which physical mechanisms are favoured during the irradiation, hence impacting on the growth of dislocations in the fuel bulk. The correlations, in the Arrhenius form, are [11]:

$$D_v = 3.7 \cdot 10^{-7} \exp\left(-\frac{2.4\,(\mathrm{eV})}{k_B T}\right) \tag{1}$$

$$D_i = 2.5 \cdot 10^{-8} \exp\left(-\frac{0.6\,(\mathrm{eV})}{k_B T}\right) \tag{2}$$

Within the range of temperature 100÷1100°C, Eq.(1) and Eq.(2) always return $D_i >> D_v$, indicating that the interstitials diffuse much faster than vacancies; this discrepancy then decreases as the temperature increases.

[1]This approximation is taken at the single-grain level, where it is reasonable to assume uniformity conditions due the magnitude of fission rate and temperature in the fuel with respect to the grain size.

Table 1: Definition of the model state variables

	Definition	Unit
c_v	Point vacancy concentration	-
c_i	Point interstitial concentration	-
C_{vl}	Vacancy loop concentration	m^{-3}
C_l	Interstitial loop concentration	m^{-3}
R_l	Interstitial loop mean radius	m
R_p	Average pore radius	m
ρ_d	Dislocation network density	$\frac{\mathrm{m}}{\mathrm{m}^3}$

Table 2: Definition of the model coefficients

	Definition	Unit
b	Burgers vector	m
$c_v^{(eq)}$	Thermal equilibrium concentration	-
$c_v^{(ps)}$	Vacancy concentration at pore surface	-
$\dot{F}$	Fission rate	$\mathrm{m}^{-3}{\cdot}\mathrm{s}^{-1}$
L_{edge}	Length of the grain edge	m
R_{vl}	Vacancy loop mean radius	m
$Z_{v,i}$	Point defect bias factor	-
α	Recombination constant	m^{-2}
α_l	Interstitial loop nucleation constant	m^{-2}
η	Nr. of vacancies knocked out per collision	-
θ	Pore dihedral angle	-
λ	Fission fragment path	m
ξ	Vacancy cluster formation modifier	-
Ω	U vacancy volume	m^3
Ω_{vl}	Vacancy cluster mean volume	m^3

The quantities which appear in the model equations are listed in Tables 1 and 2. The complete set of ordinary differential equations is the following:

$$\dot{c_v} = -\left(k_v^2 + k_{v,gb}^2\right) D_v c_v - \alpha D_i c_i c_v + (1-\xi)\, K - K_l + K_p + K_b + K_{te} \tag{3}$$

$$\dot{c_i} = -\left(k_i^2 + k_{i,gb}^2\right) D_i c_i - \alpha D_i c_i c_v + K + K_l - K_d + K_{fd} \tag{4}$$

$$\dot{C_{vl}} = +\frac{\xi K}{\Omega_{vl}} - \frac{2\pi R_{vl} C_{vl}}{\Omega_{vl}} \cdot \left[Z_i D_i c_i - Z_v D_v \left(c_v - c_v^{(eq)}\right)\right] \tag{5}$$

$$\dot{C_l} = \frac{\alpha_l D_i}{\Omega} c_i^2 - K_l - K_{fd} + \frac{4C_l}{bR_l}\left[Z_i D_i c_i - Z_v D_v \left(c_v - c_v^{(eq)}\right)\right] \tag{6}$$

$$\dot{R_l} = \frac{1}{b}\left[Z_i D_i c_i - Z_v D_v \left(c_v - c_v^{(eq)}\right)\right] \tag{7}$$

$$\dot{\rho_d} = \frac{d\left(2\pi R_l C_l\right)}{dt} \tag{8}$$

$$\dot{R_p} = \frac{1}{R_p}\left[D_v\left(c_v - c_v^{(ps)}\right) - D_i c_i\right] + - 2\Omega \dot{F} \lambda \eta \max\left(0, 1 - \frac{2R_p \sin\theta}{L_{edge}}\right) \tag{9}$$

On the right end side of Eq.(3) Eq.(4), the first term contains the total sink strengths of vacancies and interstitials towards extended defects k_v^2 $\left(\mathrm{m}^{-2}\right)$ and k_i^2 $\left(\mathrm{m}^{-2}\right)$, while $k_{v,gb}^2$ $\left(\mathrm{m}^{-2}\right)$ and $k_{i,gb}^2$ $\left(\mathrm{m}^{-2}\right)$ are respectively the grain boundary sink strengths for vacancies and interstitials; the second term refers to vacancy-interstitial recombination; the third term describes the Frenkel pair generation induced by irradiation characterised by the defect production rate K $\left(\mathrm{s}^{-1}\right)$, where in the case of Eq.(3) a certain fraction of the produced vacancies ξK $\left(\mathrm{s}^{-1}\right)$ are removed to form vacancy loops, whose contribution appears in the first term of Eq.(5). The rate K_p $\left(\mathrm{s}^{-1}\right)$ in Eq.(3) indicates the vacancies emitted per second as a result of knockout of pores by the fission fragments impinging the pores; such effect has an impact on the pore size, which is accounted in the second term of Eq.(9). Similarly, K_b $\left(\mathrm{s}^{-1}\right)$ represents the knockout of bubbles by the fission fragments impinging the bubbles, however the bubble radius is kept constant for simplicity. The rate K_l $\left(\mathrm{s}^{-1}\right)$ in Eq.(3), Eq.(4) and Eq.(6) refers to loss of point vacancies which are being absorbed by interstitial loops. Eq.(3) is completed with K_{te} $\left(\mathrm{s}^{-1}\right)$, defining the vacancy thermal production. In this model, an interstitial loop is assumed to be formed with the clustering of di-interstitials: the fifth term of Eq.(4) and the first term of Eq.(6) describe the decrease of single interstitials due to formation of interstitial loops. The rate K_{fd} $\left(\mathrm{s}^{-1}\right)$ in Eq.(4) and Eq.(6) expresses the increase in interstitial concentration as a consequence of fission damage to interstitial loops. The second term of Eq.(5) follows the absorption of point defects, where the expression in the square brackets, with the negative sign, imposes that a flow of interstitials will diminish the vacancy loop concentration, while a flow of vacancies will enhance it. Similar formulations affect the size of interstitial loops in Eq.(6) and pores in the first term of Eq.(9). Finally, Eq.(8) accounts for generation of dislocation networks by the accumulation of loops.

3. Case study results

The model has been applied for a set of fuel conditions which are normally encountered for operational light water reactors. In order to predict the onset of HBS, the model computes the dislocation density for temperatures between 100°C and 1100°C for prolonged irradiation times. In this way, it is possible to inspect the model applicability not only to conventional operating temperatures but also to fuel temperature conditions for novel designs which are outside the calibration range set by [6], such as those envisioned for SMRs for heat production.

The total dislocation density evolution is shown in Figure 1: ρ_{tot} consists in the sum of the dislocation loop density ρ_l (interstitial prismatic) and the dislocation network density ρ_d. The total dislocation density presents an increasing trend, steeply increasing at the beginning and then almost saturating throughout most of the irradiation time; the values obtained for ρ_{tot} span between $10^{14} \div 10^{16} \frac{m}{m^3}$, in line with the predictions by models [10] [11]. As expected, the dislocation density is higher at higher burn-ups and there is a noticeably high density at low temperatures. Nevertheless, if it is true that ρ_{tot} grows at all temperatures, such increase is not monotonic in

the considered range.
In addition to this preliminary evaluation, a comparison with experimental data by [6] was performed in Figure 2. The case study results at 700°C are displayed with a dashed curved together with the six experimental points: the predictions approach correctly the data extrapolated at lower burnups, but underestimate those above 40 GWd/t.
In order to perform a better prediction of the latter data points and to achieve a monotonic decrease in dislocation density with increasing temperatures, a parameter optimisation was performed. Among the model equation rates and sink strengths, the choice fell either on quantities with less physical meaning or those which could be varied over a wider range of values such to be sufficiently impactful in the new projection. These are: the recombination radius r_c, the number of defects produced in the fission track z, the bias correction factor ε, the fraction of vacancies forming clusters ξ and the number of vacancies knocked out from a pore per collision η. The model fitting with the experimental data consisted in the minimization of the residuals $\left(\rho_{tot}^{measured} - \rho_{tot}^{model}\right)$ through the least squares method. This procedure returned the following values: $r_c = 7.5 \cdot 10^{-10}\, m$, $z = 1.0 \cdot 10^4, \varepsilon = 0.024$, $\xi = 8.3 \cdot 10^{-5}$, $\eta = 10$. The model prediction after the parameter optimization is depicted with a solid line in Figure 2: the results are in reasonable agreement with the experimental data at all burn-ups within the considered range, including those at $bu > 40$ GWd/t when fuel restructuring is consistent. Moreover, above 800°C, fitting induced the ρ_{tot} to decrease as the temperature rises, approximately after four years of irradiation (Figure 3). Neverthe-

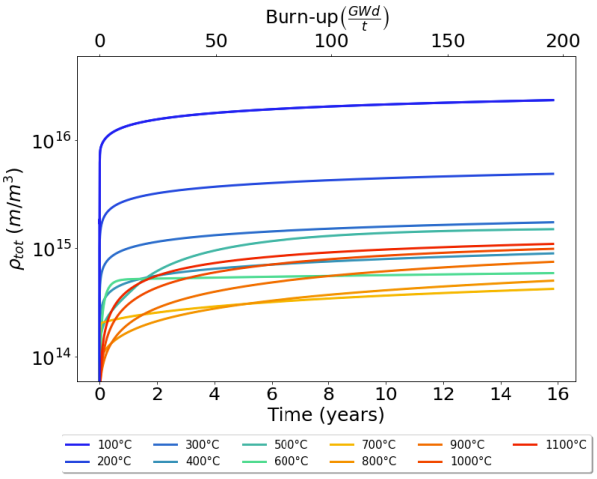

Figure 1: Evolution of the total dislocation density for the considered case study.

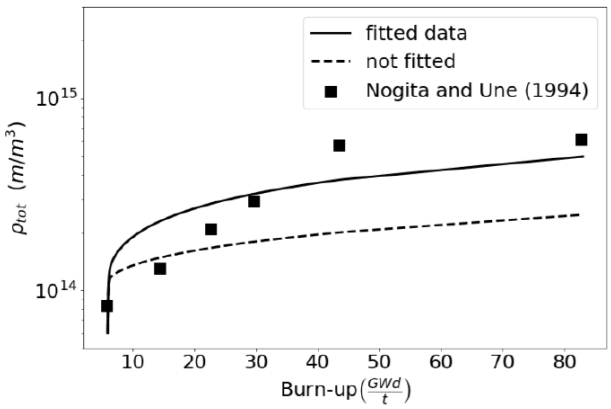

Figure 2: Comparison with experimental data by Nogita and Une at 700°C.

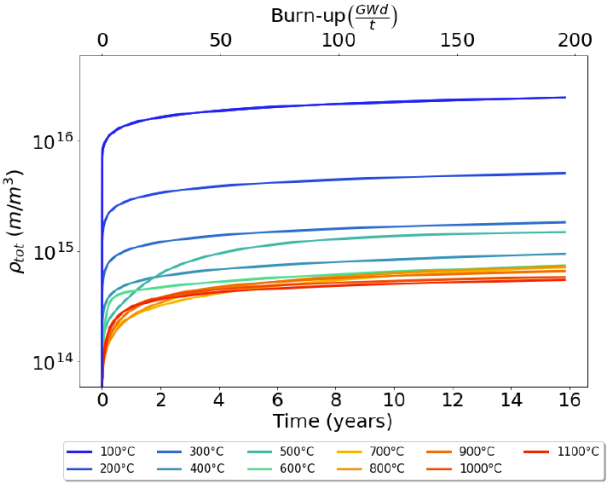

Figure 3: Evolution of the total dislocation density after parameter optimization.

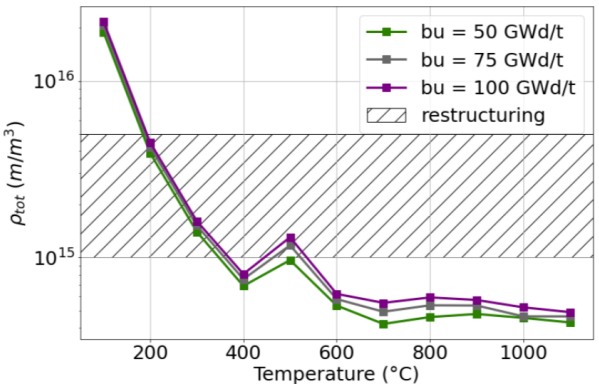

Figure 4: Evolution of ρ_{tot} against temperature after parameter fitting with experimental data. The restructuring limits are the same ones as [7].

less ρ_{tot} still does not increase monotonically with temperature, largely because of the sharp increase at around 500°C. A possible interpretation for this peak lies in the fact that, in the conditions set by this case study, between 400÷600°C the system dynamics particularly favours vacancy clustering: indeed, the concentration of point vacancies finally reaches saturation as their higher mobility allows them to aggregate more easily, thus driving lower probability of interaction with interstitials and interstitial loops. From this it conveys that more interstitials will be available to form loops, and the presence of dislocation loops will be less compromised by the action of point vacancies; the increasing C_l then immediately reflects in increasing ρ_{tot}.

In Figure 4, the ρ_{tot} is represented at different burn-ups: as expected, the total dislocation density is higher at higher bu and there is a noticeably high density at low temperatures. Generally, fuel restructuring is accepted within a range of values of dislocation density (as done in MARGARET) that here is taken as $1 \div 5 \cdot 10^{15}$ $\frac{m}{m^3}$. Below 200°C the results obtained for ρ_{tot} are above this range, hence the fuel is locally completely restructured. This is a significant result that indicates there might be a substantial formation of HBS in the potential deployment of novel SMRs for heat production.

4. Surrogation of the model

The possible implementation of the presented model into fuel performance codes requiring an evaluation of the dislocation density may result difficult, especially in view of the challenging mathematical formulation of the model equations [12]. A useful step in this regard consists in the surrogation of the model, which approximates the underlying behaviour of the rate equations in a given domain with the advantage of reducing the computational time required to reproduce the solutions. The surrogate is able to efficiently replace the original model solution thanks to a neural network constructed on a training dataset of input-output pairs from full simulations of the physics-based model [13] [14]. Indeed, the original mathematical expressions were smoothed out from discontinuities also in view of the network training needed for surrogation.

For a first network acting as a surrogate model, the total dislocation density is taken as output, as this state variable is the main reference indicator for HBS restructuring; still, rather than generating the integrated value ρ_{tot}, the time derivative $\dot{\rho_{tot}}$ is preferred because it can be inserted directly in the fuel performance codes (FPCs) solvers. In order to build a surrogate able reproduce accurately the original model, it is first necessary to generate a data set characterized by the input values varied over a certain range of possible operating fuel conditions with their corresponding output. The three selected inputs are:

- Fission rate $\dot{F} = \left[5.0 \cdot 10^{18}; 5.0 \cdot 10^{19}\right]$ $\mathrm{m}^{-3} \cdot \mathrm{s}^{-1}$.
- Temperature $T = [100; 1200]$°C.
- Burn-up $bu = [0; 200]$ GWd/t.

Given this input domain, a latin hypercube sampling of 10000 data points $\left(\dot{F}, T, bu\right)$ was performed. Each point was then given to the original model to generate the corresponding value of the time derivative of the total dislocation density. The final outcome consists in a dataset defined by $\left(\dot{F}, T, bu, \dot{\rho_{tot}}\right)$ points, which were further divided in the three smaller lists of training (making up 60% of points), validation (20%) and test (20%). The final structure of the surrogate is depicted in Figure 5: the 3 input - 1 output network is intermediated by one hidden layer that eleborates the given data, populated by 32 nodes exploiting the activation functions ReLU+Linear.

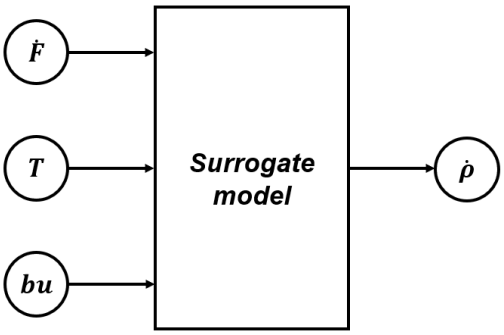

Figure 5: Schematic representation of the surrogate model.

Figure 6 gives indications about the network

performance: subfigure 6a indicates that the base ten logarithm of the mean square error (MSE) between network estimations and training-validation outputs stabilize within -3.5 and -4.5, i.e. a MSE approximately between 0.03% and 0.003%, suggesting the network is able to return valid predictions with respect to the original model outputs. In addition, subfigure 6b represents a reasonable response of the surrogate towards test output values, as the points tend to gather along the plot bisector. The estimations become less accurate for the highest values of the total dislocation density (> 0.8) due to the fact that the training dataset contained few of such high value $\dot{\rho_{tot}}$, therefore the network is less trained to predict them.

5. Conclusions

The present work consisted in the development of a physics-based model that considers the interaction and evolution of point and extended defects in UO_2 under irradiation. The main focus of the study was directed towards the evolution of dislocation density ρ_{tot}, since dislocations are microstructural features playing a crucial role in fuel restructuring and in the resulting emergence of HBS. The model was conceived to substitute correlations such as the one used in MARGARET for applications that go beyond their calibration range. The proposed model thoroughly incorporates and summarizes most of the advancements in the subject available in literature, ensuring a comprehensive representation of key phenomena. It is distinguished by a complex yet physics-based description and it serves as a versatile solution suitable for stan-

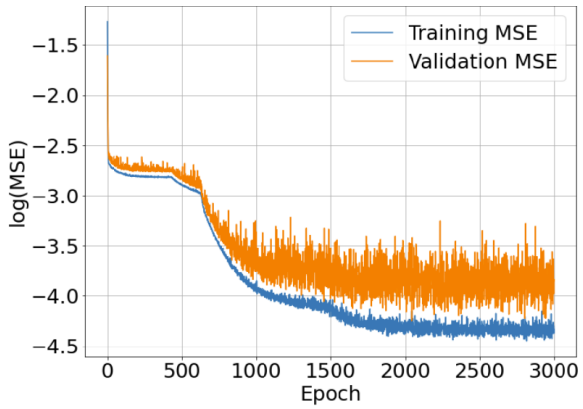

(a)

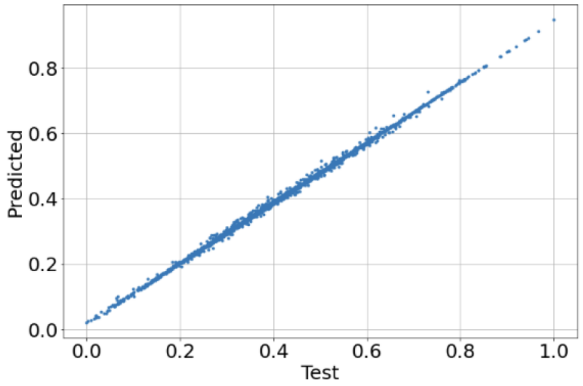

(b)

Figure 6: (6a) Comparison of the mean square error between training and validation runs; (6b) predicted values of $\dot{\rho}$ by the surrogate against the testing data.

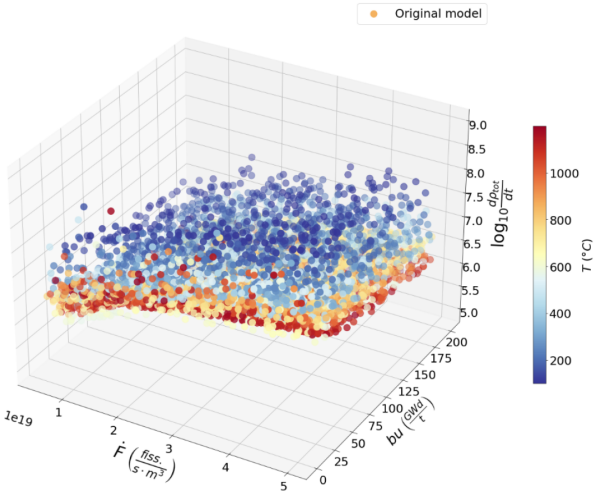

Figure 7: Original model results for the sampled input points.

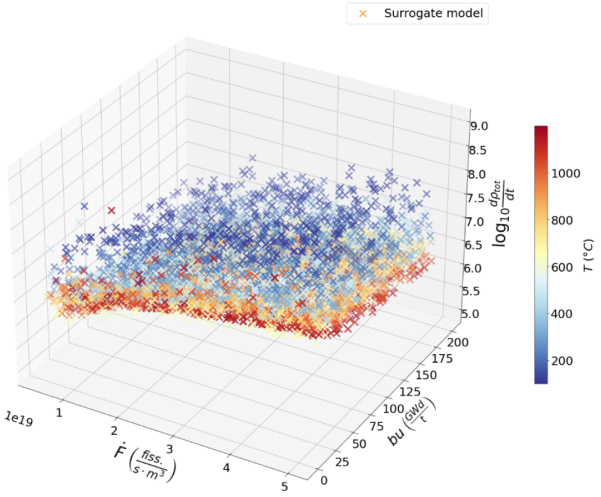

Figure 8: Surrogate model results for the sampled input points.

dalone applications or as a module within FPCs. Notably, the overall performance is enhanced by avoiding discontinuities in the equations and by specifically treating the most uncertain parameters through fitting. The model accuracy is also confirmed by validation of the results against available data: the model was already returning reasonable estimations of the total dislocation density with physically sound values of the parameters, but after the parameter optimization the model predictions improved, sensibly approaching the experimental data. Furthermore, the developed model foresees high values of dislocation density especially at low local fuel temperatures (T<250°C), suggesting substantial HBS formation that may interest sizeble portions of the fuel pellet. For the considered case study, the dislocation density evolution monotonically increases with irradiation time (or burn-up) but not with temperature, even after the fitting. Temperature dependence, in the form of uranium diffusion coefficients, heavily impacts the defect dynamics and will favour certain physical phenomena over others.

Finally, by sampling a consistent amount of total dislocation density estimations from a defined set of fission rate, temperature and burn-up values varied over large intervals, a neural network that could act as a surrogate to the original model was advanced. With respect to validation data the surrogate predictions of $\dot{\rho_{tot}}$ present a MSE $< 0.03\%$, demonstrating to mimic the original model results remarkably.

Not only does this physics-based model embed complexity of the many mechanisms occurring in irradiated fuel, but the surrogation is also designed for computational efficiency and practical usage. The surrogate model is available upon request and will be integrated both in MARGARET and SCIANTIX codes for fission gas behaviour. The increasing demand for SMRs in the future energy landscape sparks greater interest in modelling, particularly in surrogate models, devoted specifically for these reactor designs.

6. Acknowledgements

This Master's thesis work has been conducted as part of a 6-months internship at CEA Cadarache research centre and it has received funding support by the IDNES project. This work has been partially supported by the ENEN2plus project (HORIZON-EURATOM-2021-NRT-01-13101061677) founded by the European Union. This project has also received funding from the Euratom research and training programme 2021–2027 through the OperaHPC project under grant agreement n°101061453. This work has been chosen for presentation during the poster session at the NuFuel 2023 workshop. I would like to thank Professor Lelio Luzzi who kindly proposed me this subject and followed me throughout the entire research. My final thanks go to my parents and sister, for their unwavering support throughout my entire academic development.

Main references

[1] K. Lassmann et al. *Modelling the high burnup UO_2 structure in LWR fuel. J Nucl Mater*, 226(1):1–8, 1995.

[2] T. Sonoda et al. *Transmission electron microscopy observation on irradiation-induced microstructural evolution in high burn-up UO_2 disk fuel. Nucl Instrum Meth B*, 191:622, 2002.

[3] D. Baron et al. *Discussion about HBS transformation in high burn-up fuels. Nucl Eng and Tecy*, 41:119, 2009.

[4] Hj. Matzke et al. *t*emperature and fission rate effects on the rim structure formation in a uo_2 fuel with a burnup of 7.9 *J. Nucl. Mater.*, 252:71–78, 1998.

[5] M. Kinoshita. *Towards the mathematical model of rim structure formation. J Nucl Mater*, 248:185–190, 1997.

[6] K. Nogita and K. Une. *Radiation-induced microstructural change in high burnup UO_2 fuel pellets. Nucl Instrum Meth B*, B91:301, 1994.

[7] L. Noirot. *MARGARET: An Advanced Mechanistic Model of Fission Gas Behavior in Nuclear Fuel. Journal of Nuclear Science and Technology*, 2006.

[8] L. Malerba. *Multi-scale modelling of irradiation effects in nuclear power plant materials*, chapter 15. SCK CEN, Woodhead, 2010.

[9] D. Olander. *Point-defects in irradiated UO_2. J. Nucl. Mater.*, 399:236–239, 2010.

[10] M.S. Veshchunov and V.E. Shestak. *Model for evolution of crystal defects in UO_2 under irradiation up to high burn-ups. J. Nucl. Mater.*, 384:12–18, 2009.

[11] J. Rest and G.L. Hofman. *An alternative explanation for evidence that Xenon depletion, pore formation, and grain subdivision begin at different local burnups. J Nucl Mater*, 277:231–238, 2000.

[12] P. et al. Van Uffelen. *A review of fuel performance modelling. J. Nucl. Mater.*, 516:373–412, 2019.

[13] C. Wang et al. *An evaluation of adaptive surrogate modeling based optimization with two benchmark problems. Environmental Modelling & Software*, 60:167–179, 2014.

[14] S. E. Davis et al. *Efficient Surrogate Model Development: Optimum Model Form Based on Input Function Characteristics. Computed Aided Chemical Engineering*, 40:457–462, 2017.